

Supplement to:

Mass balance and area changes of glaciers in the Cordillera Real and Tres Cruces, Bolivia, between 2000 and 2016

Seehaus Thorsten¹, Malz Philipp¹, Sommer Christian¹, Alvaro Soruco², Matthias Braun¹

¹ Institute of Geography, Friedrich-Alexander-University Erlangen-Nuremberg, Wetterkreuz 15, 91058 Erlangen, Germany

² Instituto de Investigaciones Geológicas y del Medio Ambiente, Universidad Mayor de San Andrés, Calle 27 Cota Cota, La Paz, Bolivia

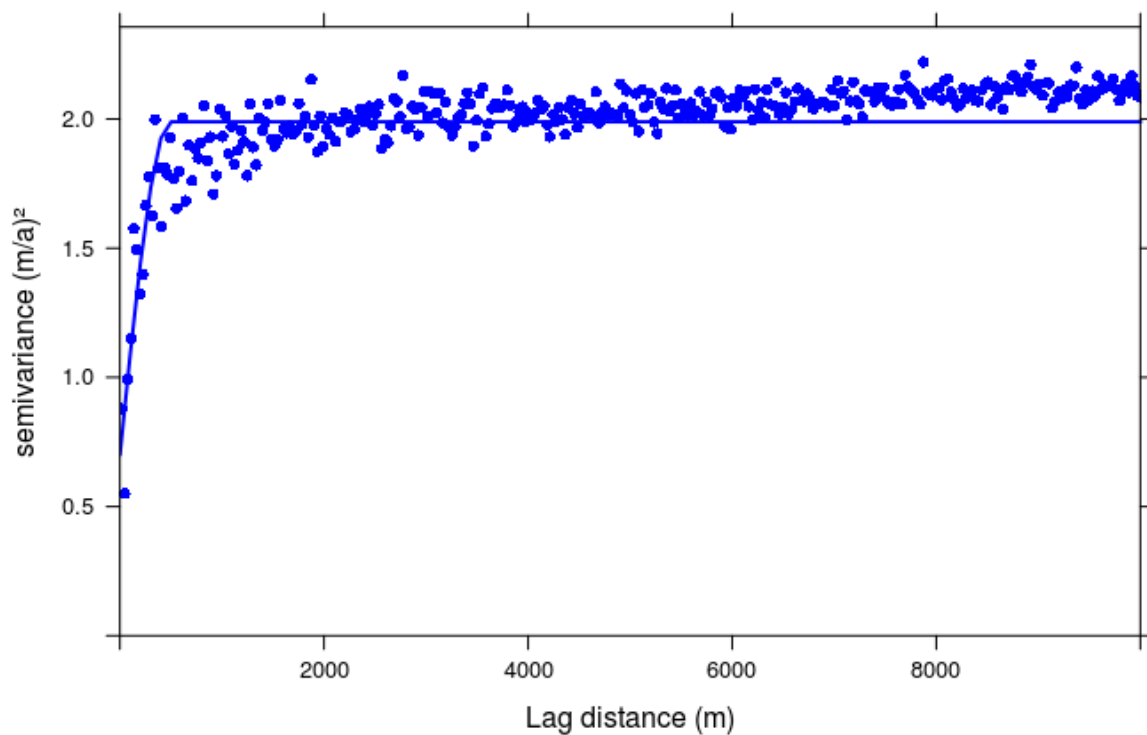


Figure S1: Semivariogram of elevation change measurements on stable ground for the period 2000-2013 (100000 random samples, 30 m distance intervals, 20 km maximum distance). Solid blue line: fitted spherical semivariogram function

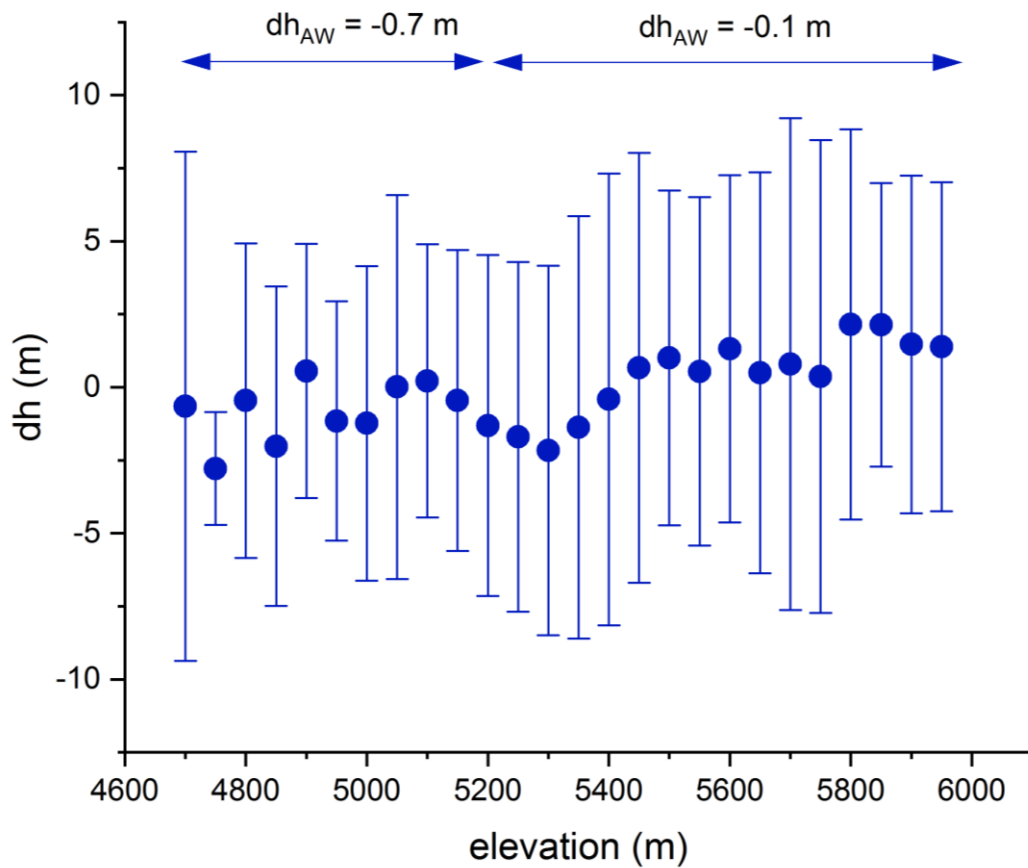


Figure S2: Hypsometric distribution of elevation changes (dh) on glacier surfaces (inventory 2013) between the Pléiades DEM and TanDEM-X DEM in 2013. dh_{AW} : area weighted mean values below and above the equilibrium line altitude (ELA) of 5144 m a.s.l. from Rabatel and others (2012). Error bars indicate NMAD of dh for each hypsometric bin.

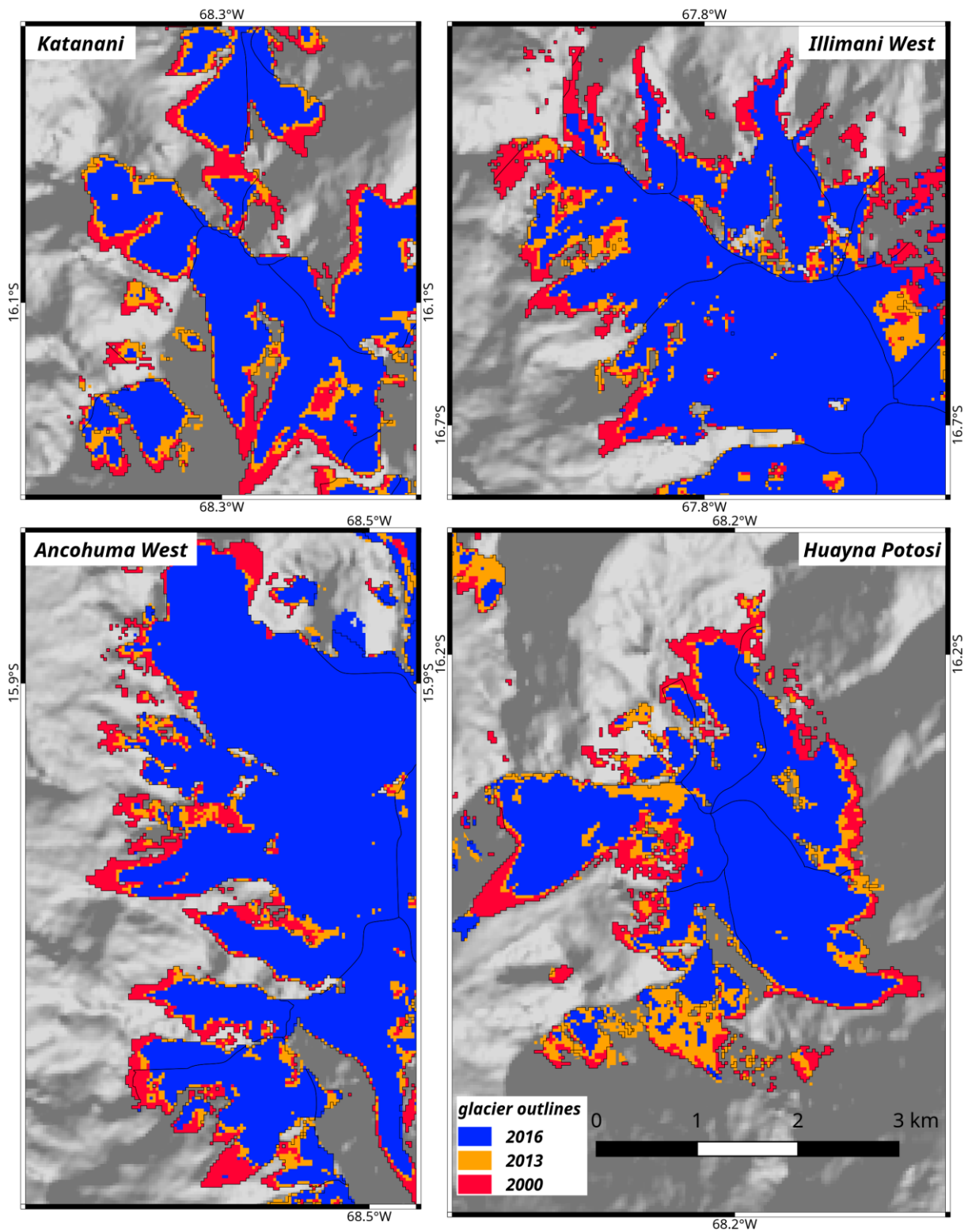


Figure S3. Glacier area changes of subsets of the study region indicated in Figure 3. Ice divides (black polygons) are from the glacier outlines in 2000. Background: SRTM hillshade © NASA 2000

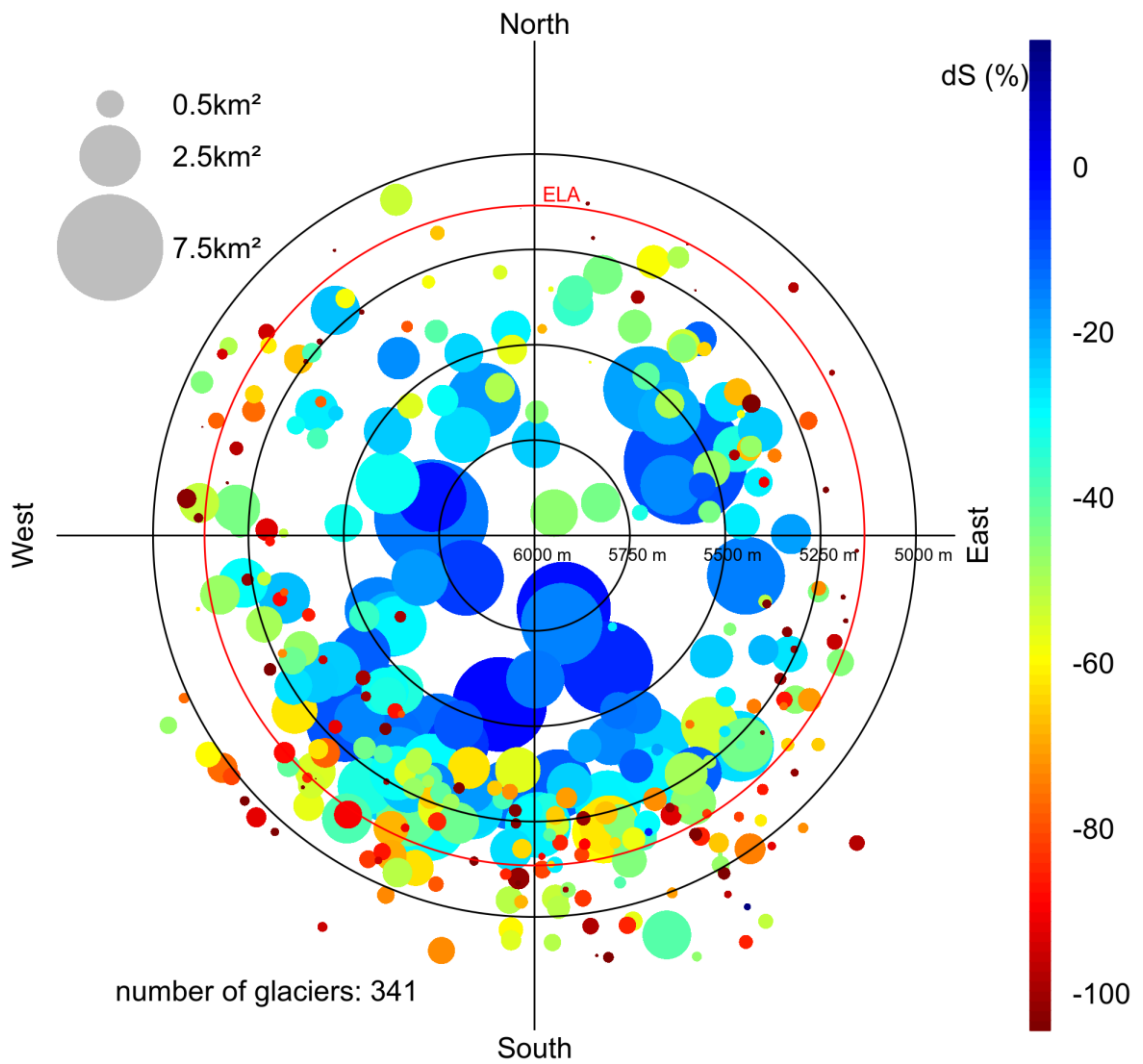


Figure S4: Relative area changes (2000-2016) of individual glaciers (dot color) plotted against glacier size (dot size), median elevation (distance from center) and mean aspect (orientation). Red circle: equilibrium line altitude (ELA) from Rabatel and others (2012).

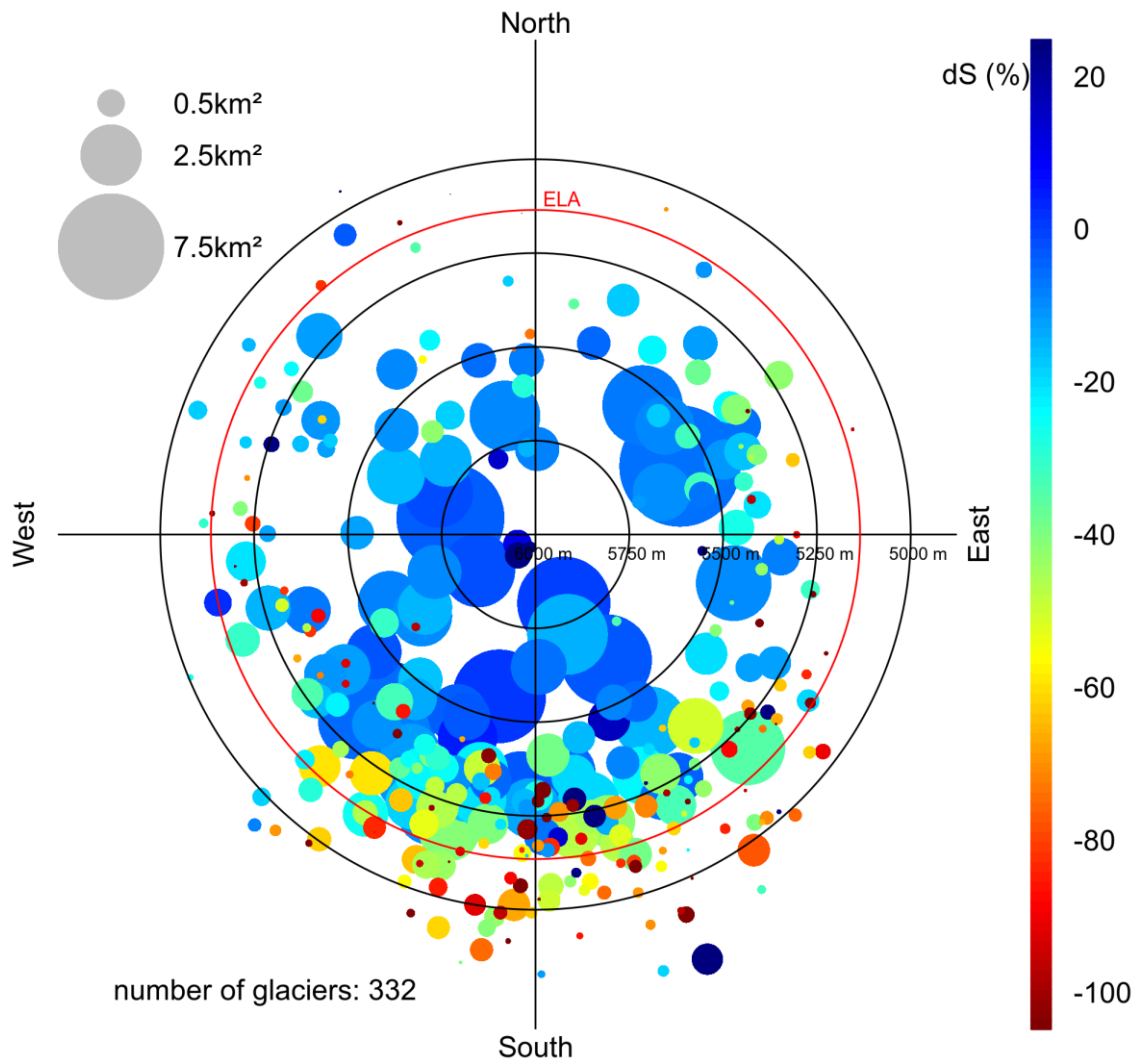


Figure S5: Relative area changes (2013-2016) of individual glaciers (dot color) plotted against glacier size (dot size), median elevation (distance from center) and mean aspect (orientation). Red circle: equilibrium line altitude (ELA) from Rabatel and others (2012).

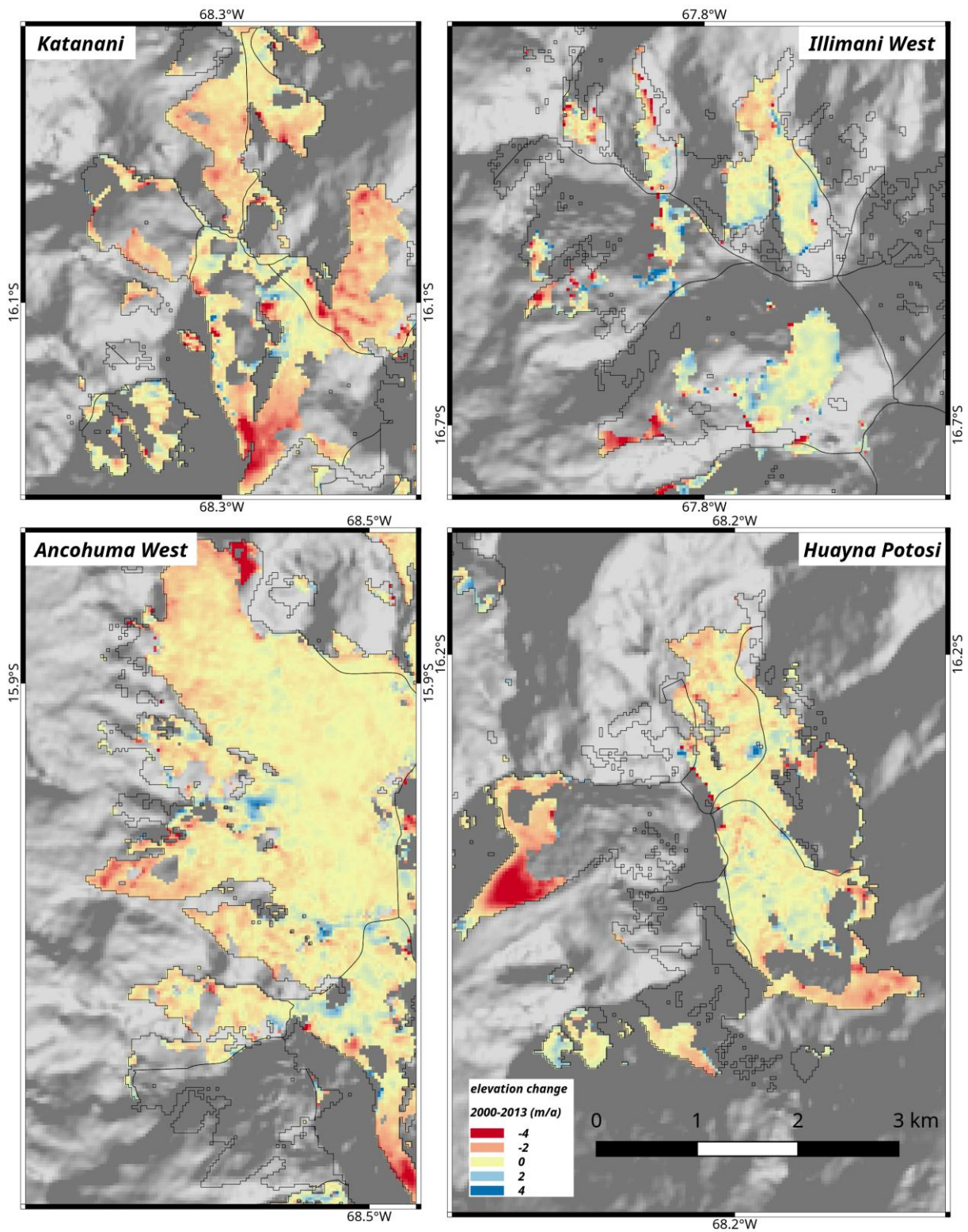


Figure S6. Glacier surface elevation changes between 2000 and 2013 of subset indicated in Figure 5. Background SRTM hillshade © NASA 2000

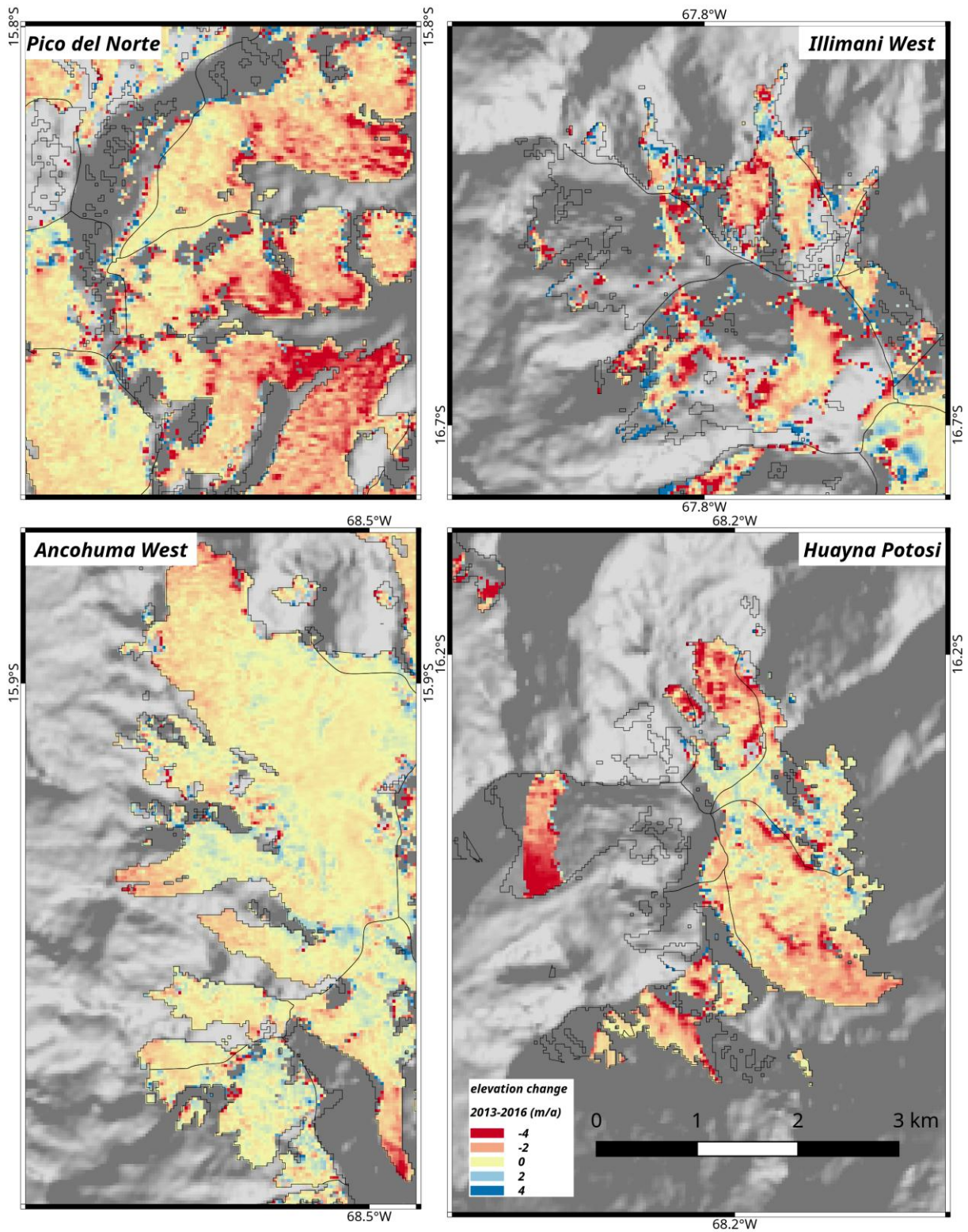


Figure S7. Glacier surface elevation changes between 2013 and 2016 of subset indicated in Figure 5. Background SRTM hillshade © NASA 2000

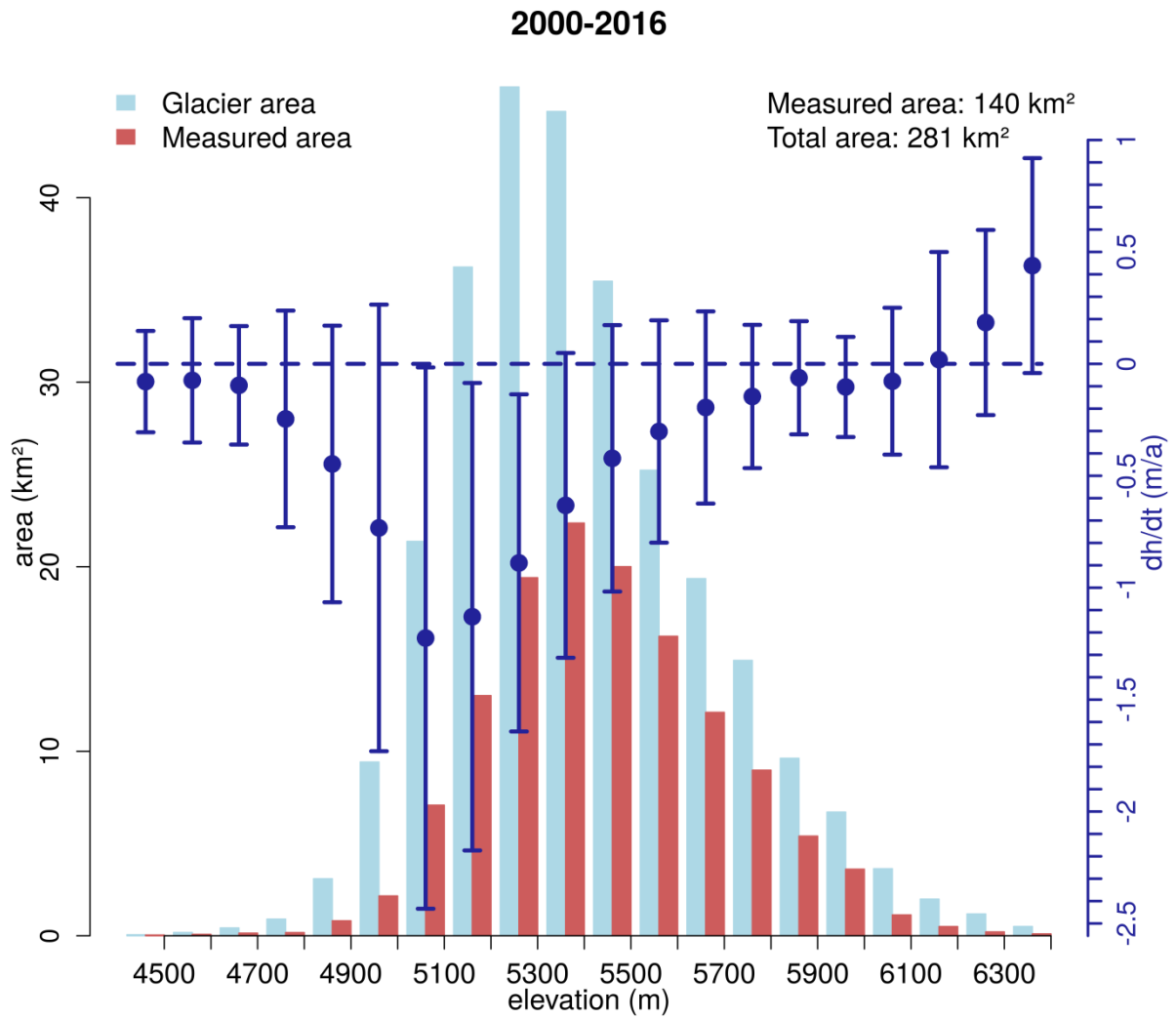


Figure S8: Hypsometric distribution of glacier area (light blue), glacier area with dh/dt measurements (red) and mean dh/dt values of each hypsometric bin for the observation period 2000-2016. Error bars indicate NMAD of dh/dt for each hypsometric bin.

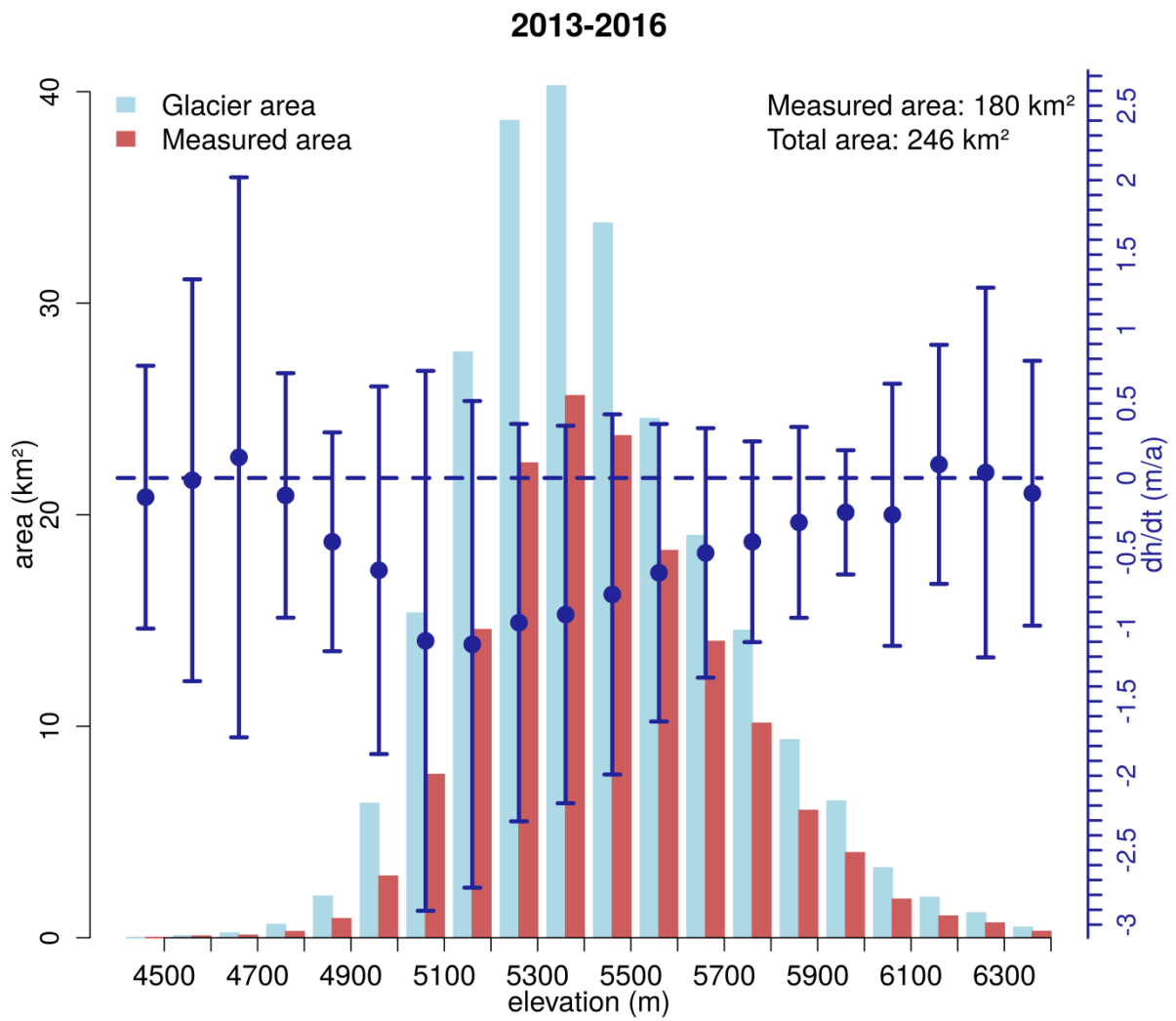


Figure S9: Hypsometric distribution of glacier area (light blue), glacier area with dh/dt measurements (red) and mean dh/dt values of each hypsometric bin for the observation period 2013-2016. Error bars indicate NMAD of dh/dt for each hypsometric bin.

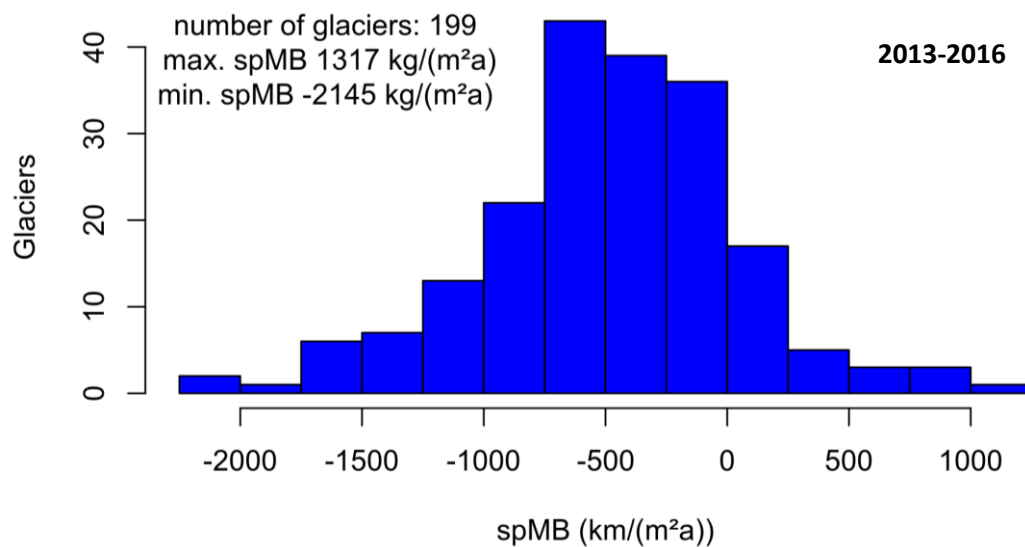
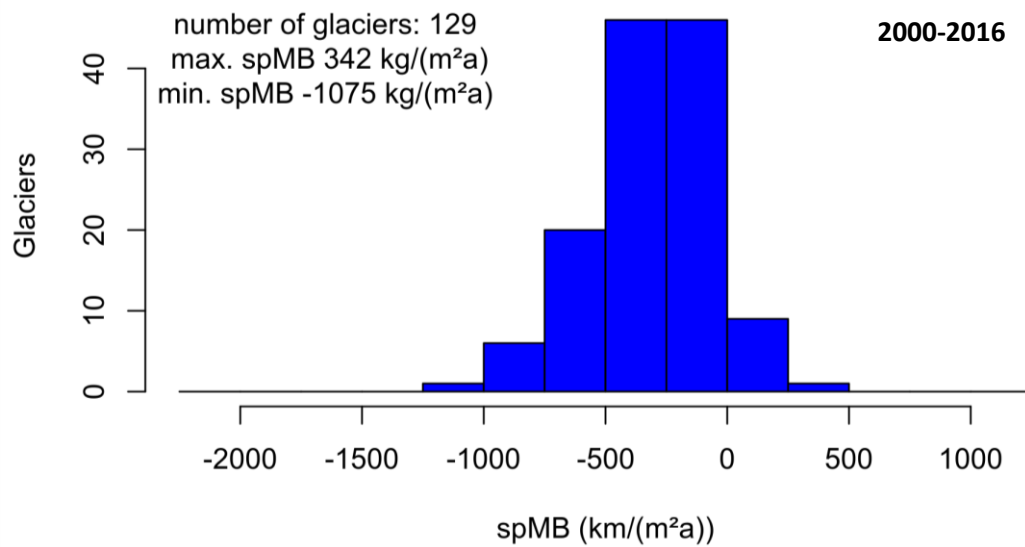
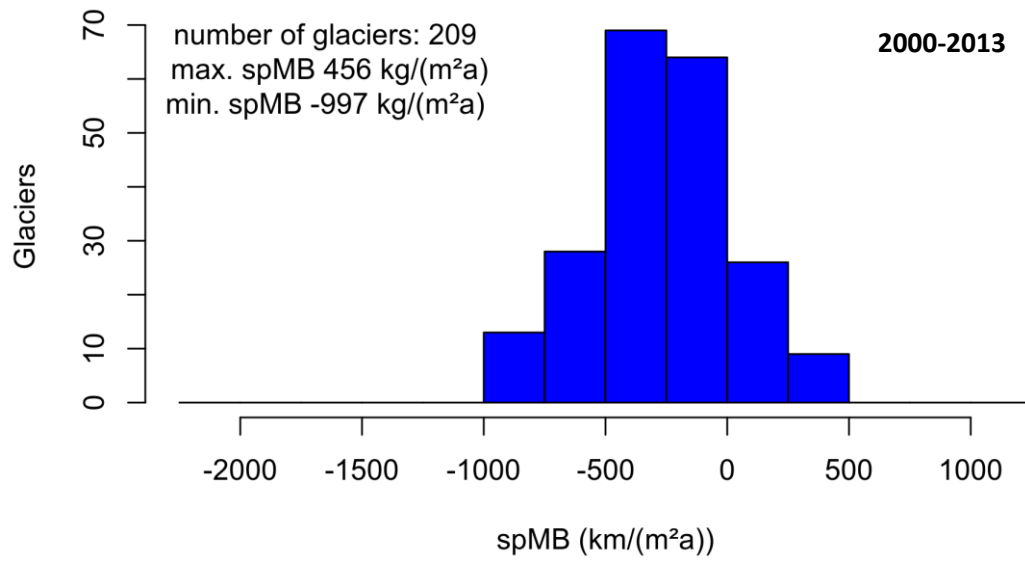


Figure S10. Specific mass balance (spMB) distributions of individual glaciers for different study periods.

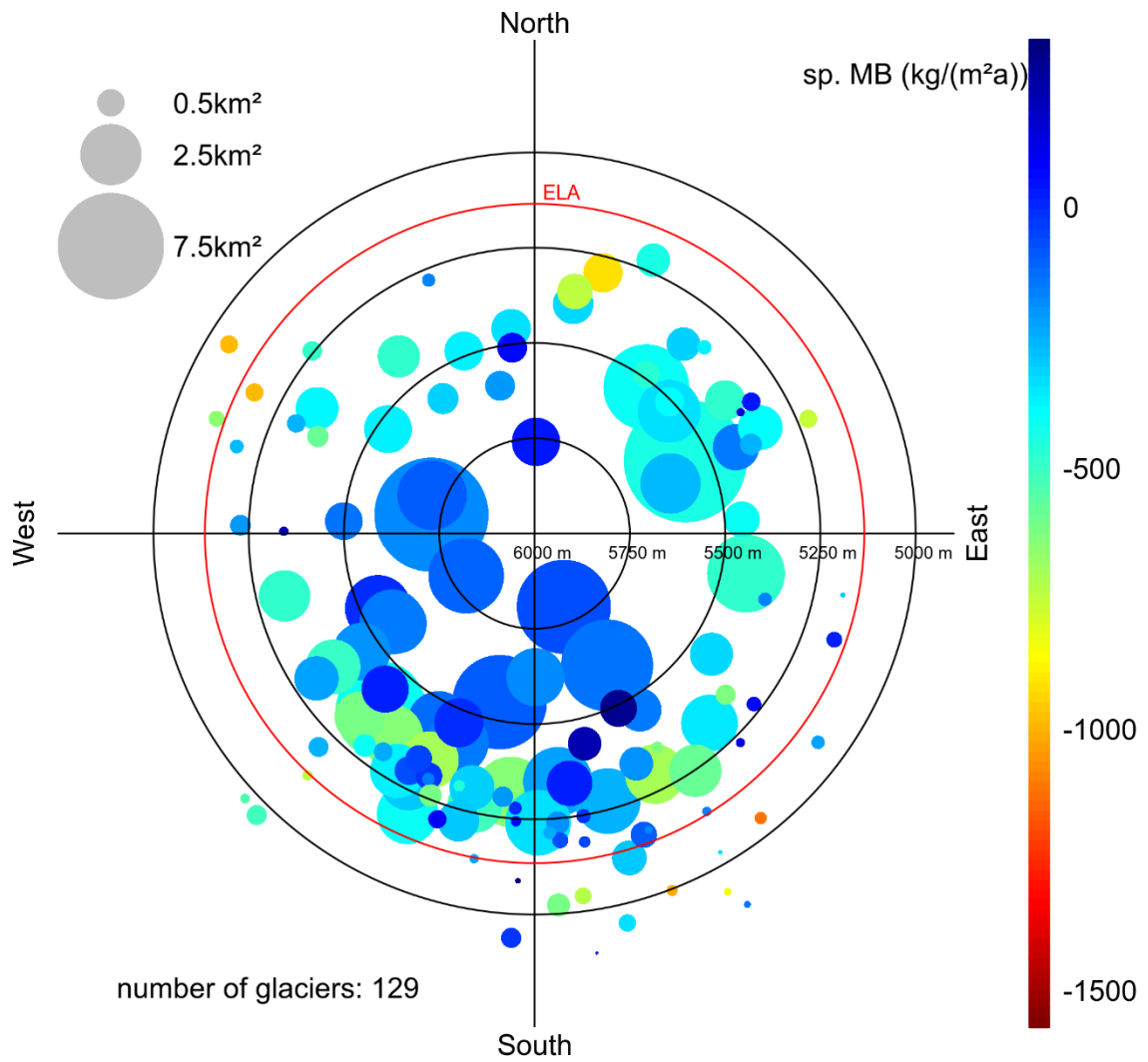


Figure S11: Specific mass balance 2000-2016 of individual glaciers (dot color) plotted against glacier size (dot size), median elevation (distance from center) and mean aspect (orientation). Red circle: equilibrium line altitude (ELA) from Rabatel and others (2012). Note: only glaciers with >40% elevation change data coverage, which is spread over >2/3 of the hypsometric distribution are included.

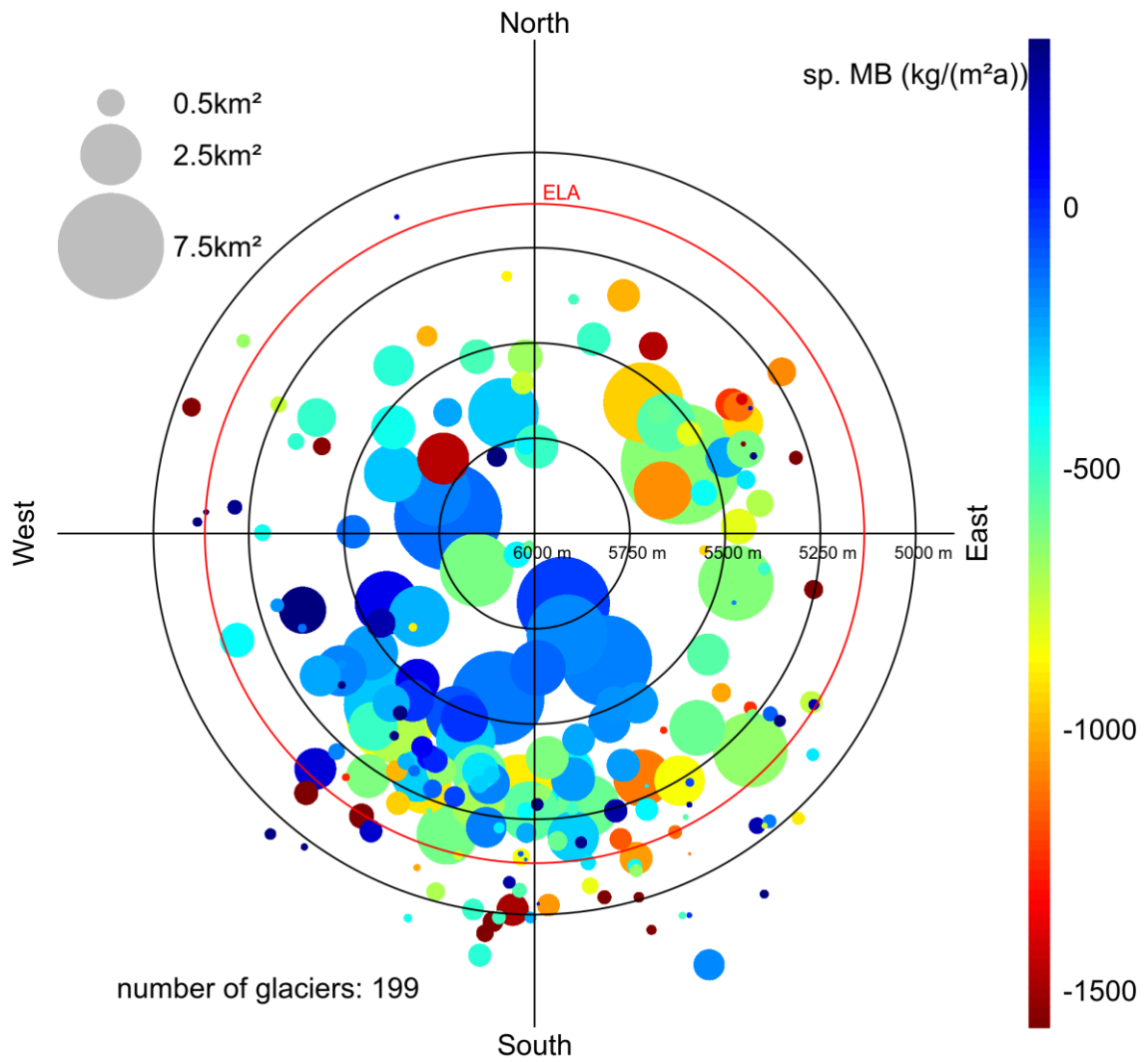


Figure S12: Specific mass balance 2013-2016 of individual glaciers (dot color) plotted against glacier size (dot size), median elevation (distance from center) and mean aspect (orientation). Red circle: equilibrium line altitude (ELA) from Rabatel and others (2012). Note: only glaciers with >40% elevation change data coverage, which is spread over >2/3 of the hypsometric distribution are included.

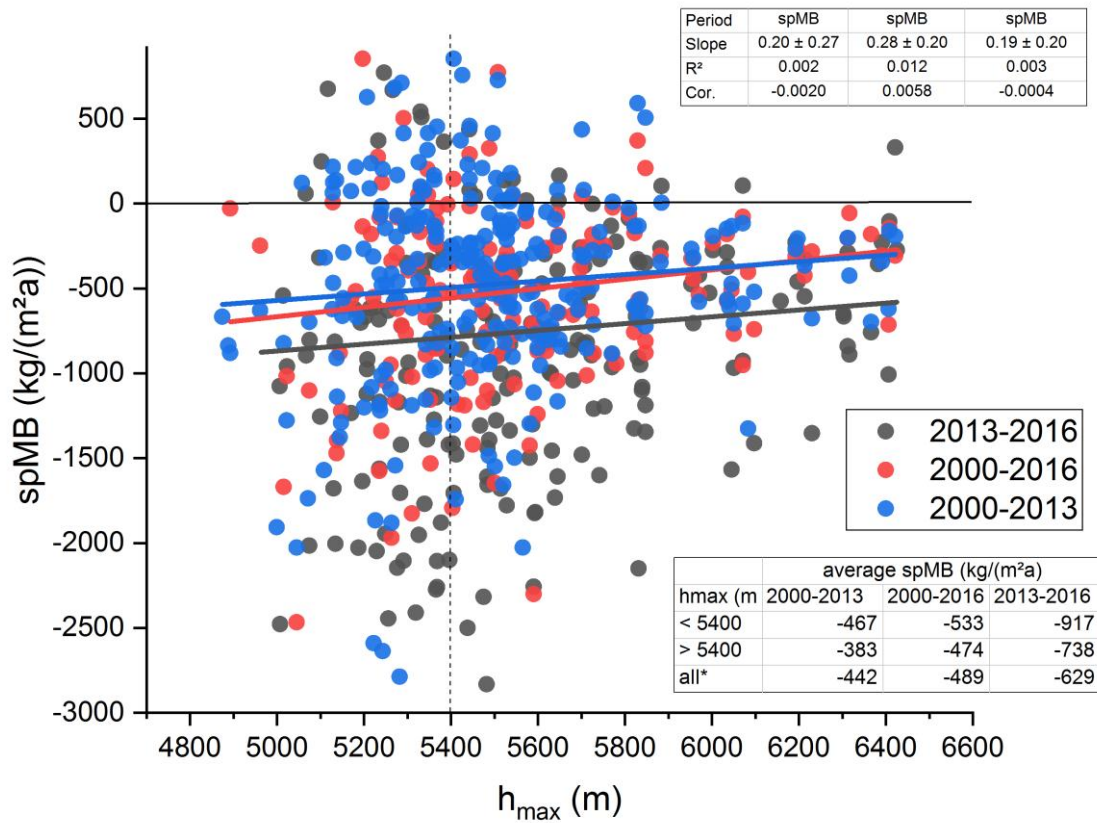


Figure S13: Specific mass balance (spMB) of individual glaciers plotted against maximum glacier elevation (h_{max}) for different periods. Solid lines: linear fit of spMB data. The table in the lower right corner summarizes the average spMB for glaciers with $h_{max} > 5400$ m and < 5400 m and for all glaciers. *area weighted average of all glaciers.

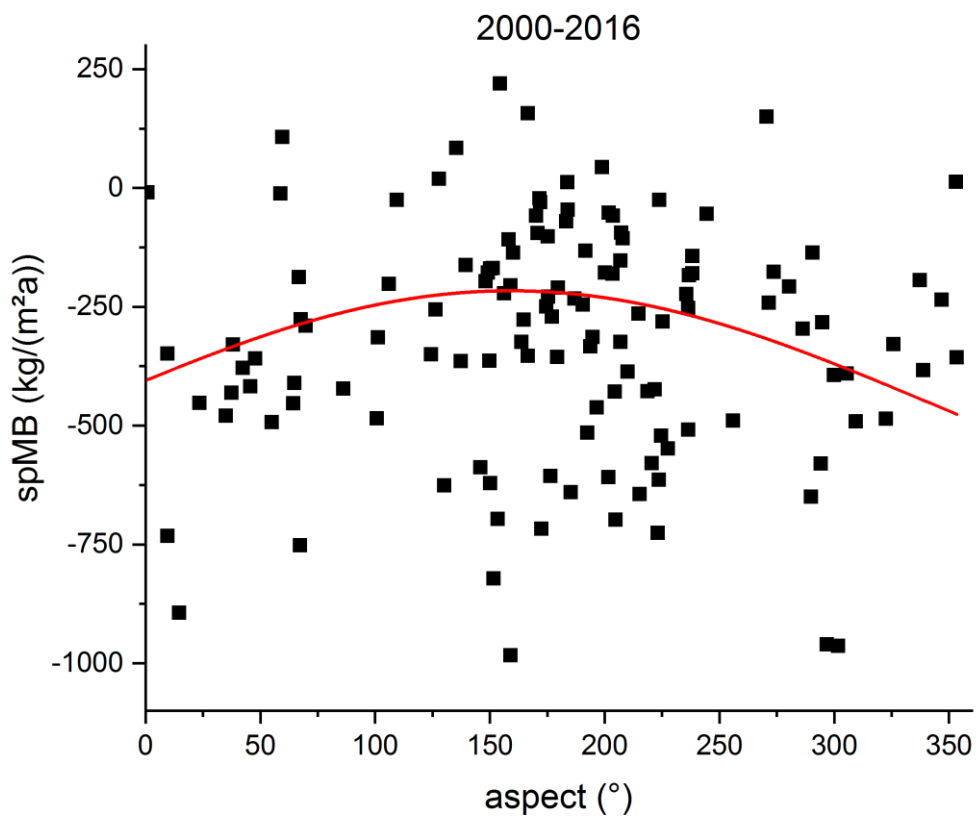
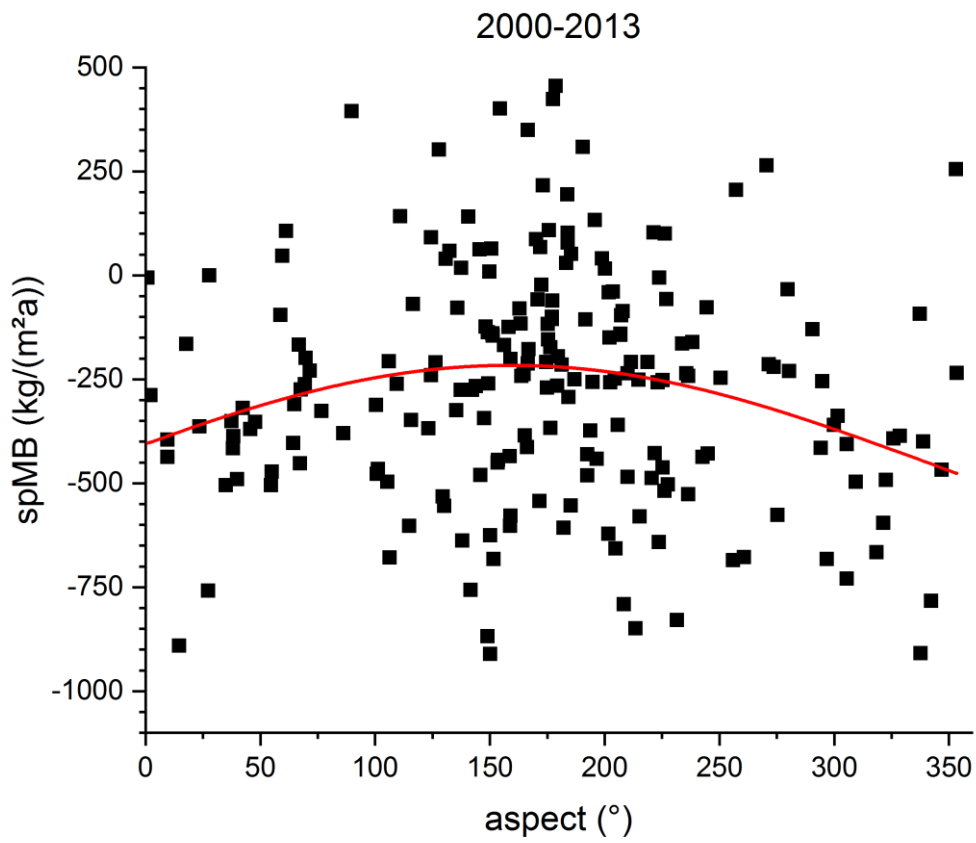


Figure S14. Specific mass balance (spMB) of individual glaciers plotted against mean glacier aspect. Red line: sinusoidal curve fitting.

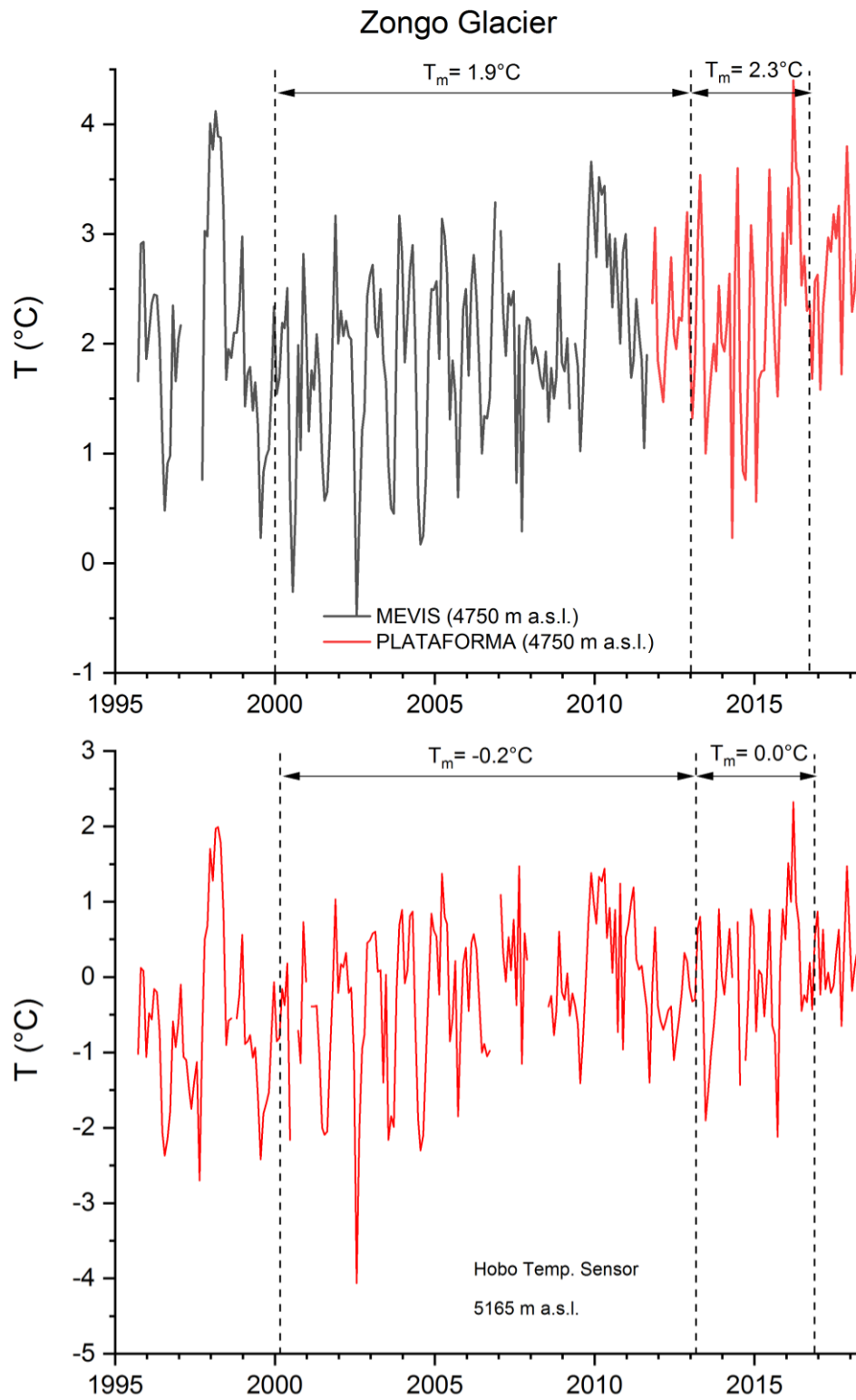


Figure S15: Temperature recordings at Zongo Glacier. Upper panel: the “Mevis” station was replaced by “Plataforma” (same elevation, 40 m distance) in 2011.

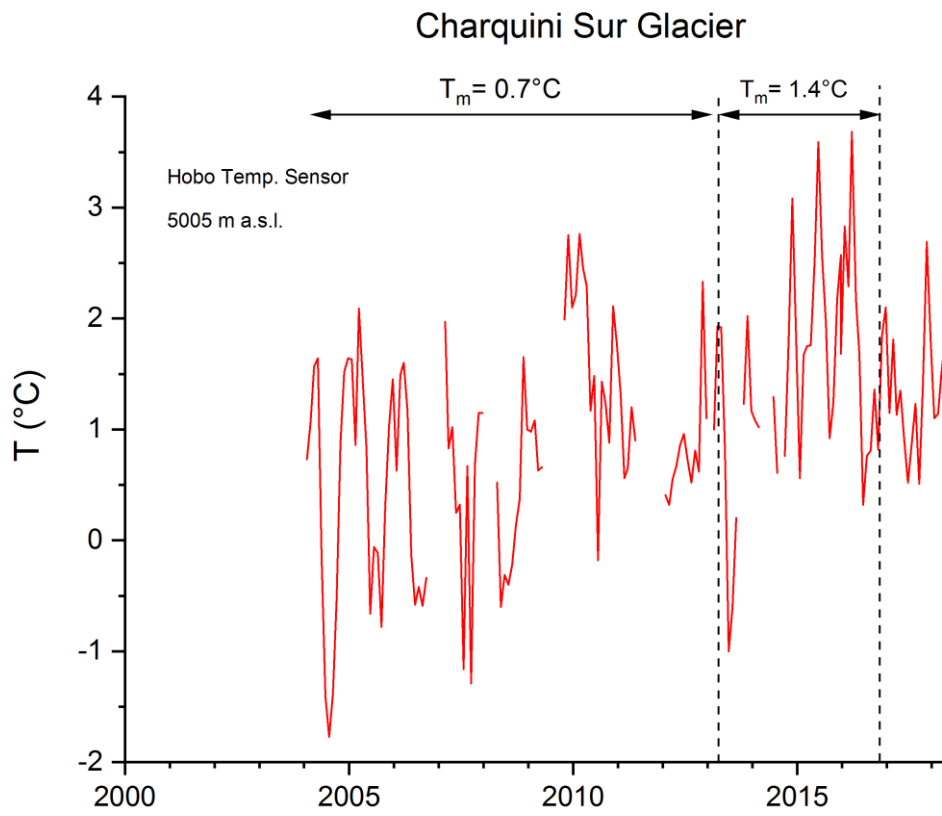


Figure S16. Temperature recordings at Charquini Sur Glacier.

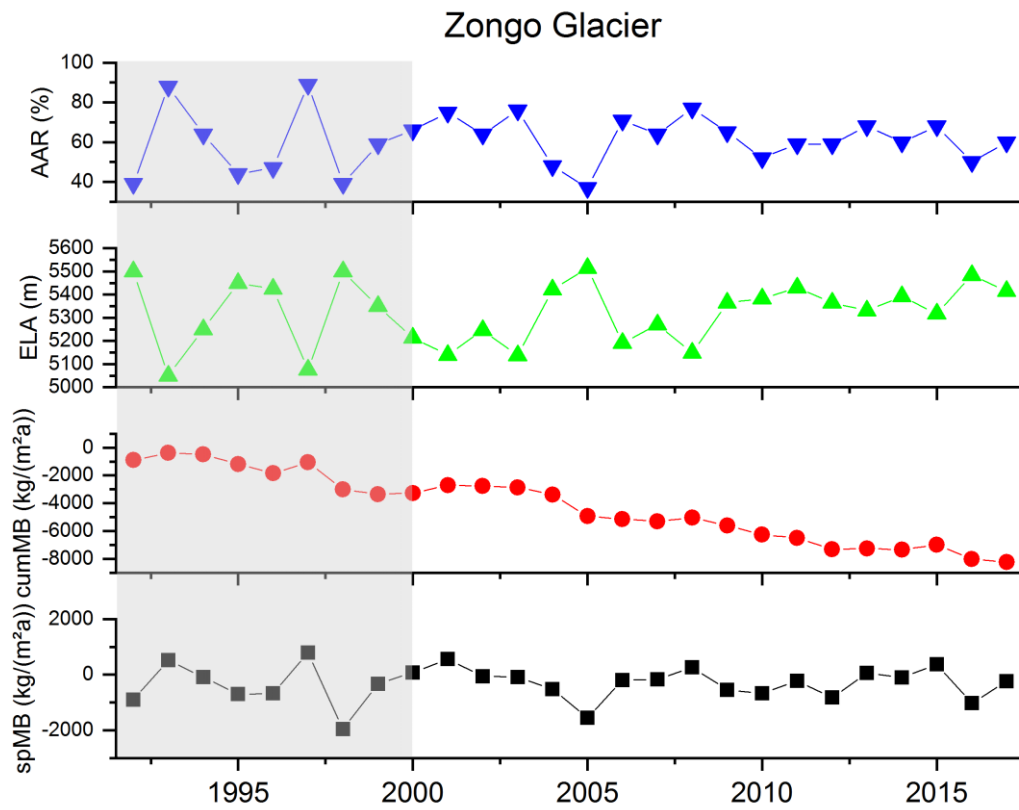


Figure S17: Temporal evolution of accumulation-area-ratio (AAR), equilibrium line altitude (ELA), cumulative mass balance (cumMB) and specific mass balance (spMB) at Zongo Glacier obtained by glaciological measurements.

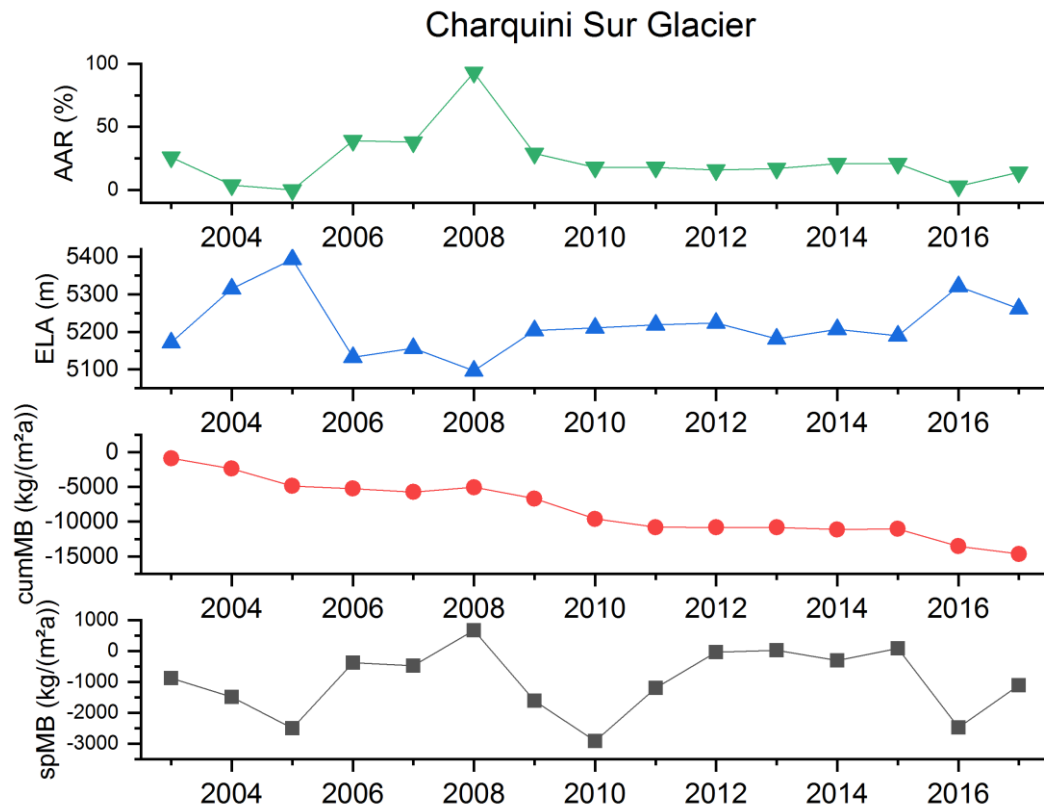


Figure S18: Temporal evolution of accumulation-area-ratio (AAR), equilibrium line altitude (ELA), cumulative mass balance (cumMB) and specific mass balance (spMB) at Charquini Sur Glacier obtained by glaciological measurements.

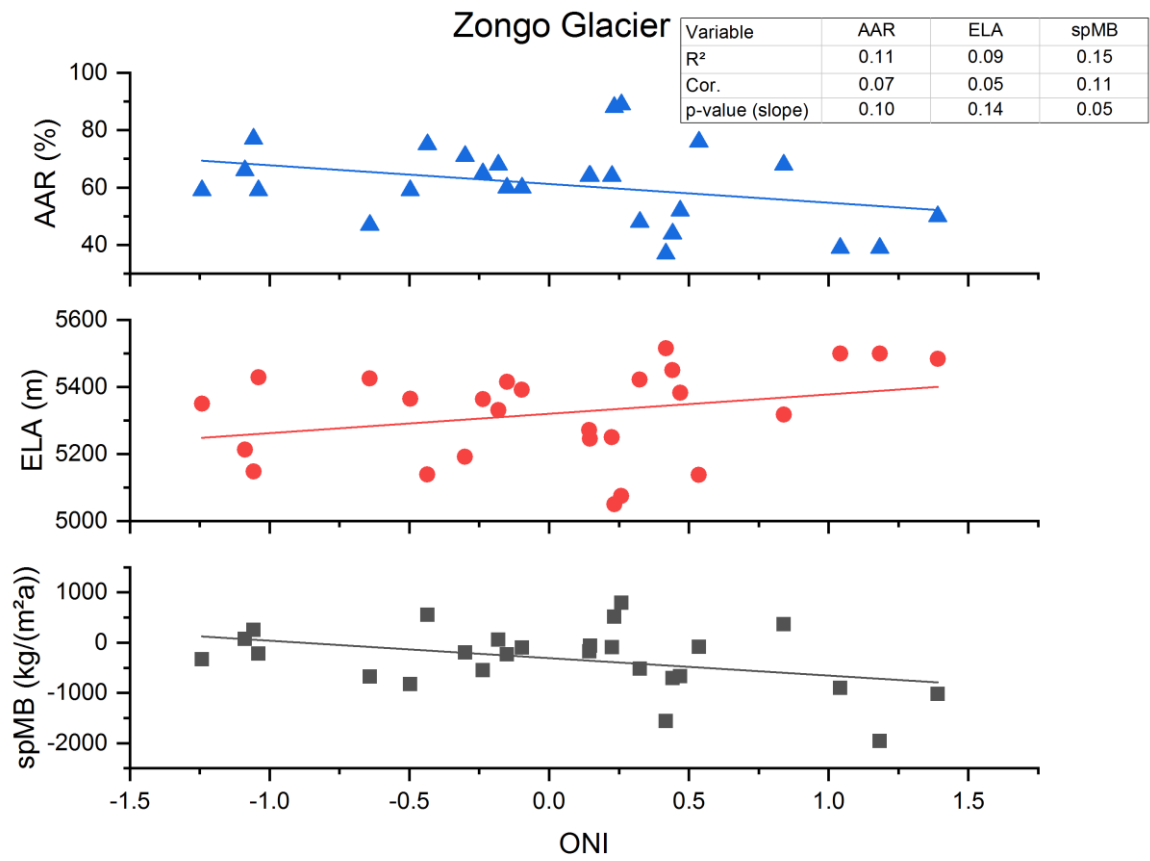


Figure S19: Accumulation-area-ratio (AAR), equilibrium line altitude (ELA) and specific mass balance (spMB) at Zongo Glacier obtained by glaciological measurements plotted against the average ONI value of the observation periods (September-August). Solid lines: linear fits of the different variables

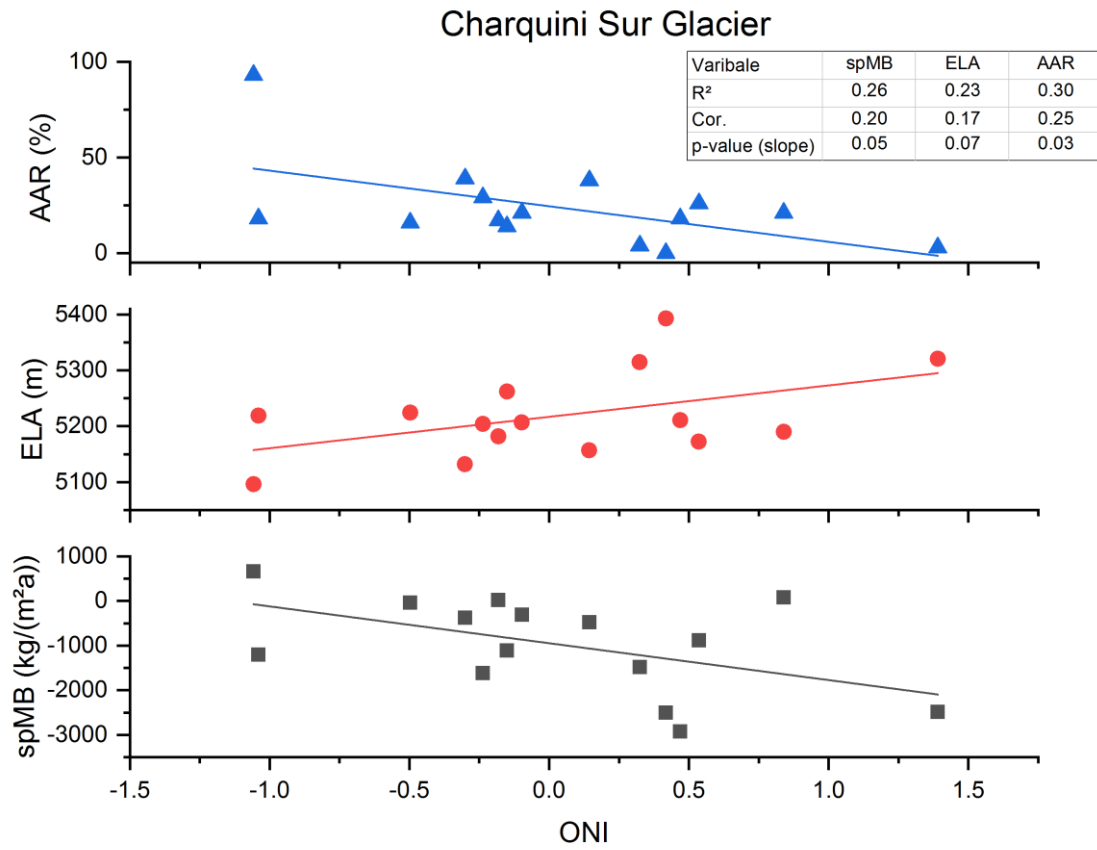


Figure S20: Accumulation-area-ratio (AAR), equilibrium line altitude (ELA) and specific mass balance (spMB) at Charquini Sur Glacier obtained by glaciological measurements plotted against the average ONI value of the observation periods (September-August). Solid lines: linear fits of the different variables

Table S1: Overview of analyzed remote sensing data

a) Landsat data sets					
Satellite	Date	Sensor	ID	Path	Row
Landsat 5	2000-07-29	TM	LT52330722000211XXX02	233	72
Landsat 5	2000-08-05	TM	LT50010712000218AAA02	1	71
Landsat 5	2000-08-05	TM	LT50010722000218AAA02	1	72
Landsat 8	2013-08-18	OLI	LC82330722013230LGN01	233	72
Landsat 8	2013-09-26	OLI	LC80010712013269LGN01	1	71
Landsat 8	2013-09-26	OLI	LC80010722013269LGN01	1	72
Landsat 8	2016-07-25	OLI	LC82330722016207LGN00	233	72
Landsat 8	2016-08-01	OLI	LC80010712016214LGN00	1	71
Landsat 8	2016-08-01	OLI	LC80010722016214LGN00	1	72

b) TanDEM-X data sets				
Date	Pass dir.	Scenes	Rel. Orbit	Strip
2013-01-05	D	2	111	85
2013-01-16	D	2	111	75
2013-01-21	D	1	20	55
2013-02-14	A	2	58	55
2013-02-25	A	3	58	45
2013-03-06	D	2	20	45
2013-03-08	A	3	58	35
2013-03-17	D	2	20	25
2013-03-19	A	2	58	25
2016-09-13	D	1	20	10
2016-09-15	A	2	58	10
2016-09-24	D	1	20	20
2016-09-26	A	1	58	30
2016-09-30	D	1	111	90
2016-10-07	A	1	58	40
2016-10-16	D	1	20	50
2016-11-13	D	1	111	80

Pass direction: A – ascending, D - descending

References

Rabatel A, Bermejo A, Loarte E, Soruco A, Gomez J, Leonardini G, Vincent C and Sicart JE (2012) Can the snowline be used as an indicator of the equilibrium line and mass balance for glaciers in the outer tropics? *J. Glaciol.* 58(212), 1027–1036 (doi:10.3189/2012JoG12J027)